



Ulrike Hess, Gerd Mikolajczyk, Laura Treccani, Philipp Streckbein, Christian Heiss, Stefan Odenbach, Kurosch Rezwan

Multi-loaded ceramic beads/matrix scaffolds obtained by combining ionotropic and freeze gelation for sustained and tuneable vancomycin release

Journal Article as: peer-reviewed accepted version (Postprint)

DOI of this document* (secondary publication): <https://doi.org/10.26092/elib/2497>

Publication date of this document: 29/09/2023

* for better findability or for reliable citation

Recommended Citation (primary publication/Version of Record) incl. DOI:

Ulrike Hess, Gerd Mikolajczyk, Laura Treccani, Philipp Streckbein, Christian Heiss, Stefan Odenbach, Kurosch Rezwan,
Multi-loaded ceramic beads/matrix scaffolds obtained by combining ionotropic and freeze gelation for sustained and tuneable vancomycin release,
Materials Science and Engineering: C, Volume 67, 2016, Pages 542-553, ISSN 0928-4931,
<https://doi.org/10.1016/j.msec.2016.05.042>

Please note that the version of this document may differ from the final published version (Version of Record/primary publication) in terms of copy-editing, pagination, publication date and DOI. Please cite the version that you actually used. Before citing, you are also advised to check the publisher's website for any subsequent corrections or retractions (see also <https://retractionwatch.com/>).

This document is made available under a Creative Commons licence.

The license information is available online: <https://creativecommons.org/licenses/by-nc-nd/4.0/>

Take down policy

If you believe that this document or any material on this site infringes copyright, please contact publizieren@suub.uni-bremen.de with full details and we will remove access to the material.

Multi-loaded ceramic beads/matrix scaffolds obtained by combining ionotropic and freeze gelation for sustained and tuneable vancomycin release

Ulrike Hess^a, Gerd Mikolajczyk^b, Laura Treccani^{a,*}, Philipp Streckbein^{c,e}, Christian Heiss^{d,e}, Stefan Odenbach^b, Kurosch Rezwan^{a,f}

^a Advanced Ceramics, University of Bremen, Am Biologischen Garten 2, 28359 Bremen, Germany

^b Institute of Fluid Mechanics, Chair of Magneto-fluid dynamics, Measuring and Automation Technology, TU Dresden, George-Baehr-Strasse 3, 01069 Dresden, Germany

^c Department for Cranio-Maxillofacial and Plastic Surgery, University Hospital of Giessen-Marburg GmbH, Campus Giessen, Klinikstrasse 33, 35392 Giessen, Germany

^d Department of Trauma, Hand and Reconstructive Surgery, University Hospital of Giessen-Marburg GmbH, Campus Giessen, Rudolf-Buchheim-Strasse 7, 35392 Giessen, Germany

^e Laboratory of Experimental Surgery, Justus-Liebig-University of Giessen, Kerkrader Strasse 9, 35394 Giessen, Germany

^f MAPEX Center for Materials and Processes, University of Bremen, Am Fallturm 1, 28359 Bremen, Germany

ARTICLE INFO

Article history:

Received 30 October 2015

Received in revised form 20 April 2016

Accepted 12 May 2016

Available online 14 May 2016

Keywords:

Drug carrier

Drug release

Hydroxyapatite

Scaffold

Beads

Vancomycin

ABSTRACT

For a targeted release against bacteria-associated bone diseases (osteomyelitis) ceramic beads with a high drug loading capacity, loaded with vancomycin as model antibiotic, are synthesized as drug carrier and successfully incorporated in an open porous hydroxyapatite matrix scaffold via freeze gelation to prevent bead migration at the implantation site and to extend drug release. We demonstrate that the quantity of loaded drug by the hydroxyapatite and β -tricalcium phosphate beads, produced by ionotropic gelation, as well as drug release can be tuned and controlled by the selected calcium phosphate powder, sintering temperature, and high initial vancomycin concentrations (100 mg/ml) used for loading. Bead pore volume up to 68 mm³/g, with sufficiently large open pores (pore size of up to 650 nm with open porosity of 72%) and high surface area (91 m²/g) account likewise for a maximum drug loading of 236 mg/g beads or 26 mg/sample. Multi-drug loading of the beads/matrix composite can further increase the maximum loadable amount of vancomycin to 37 mg/sample and prolong release and antibacterial activity on *Bacillus subtilis* up to 5 days. The results confirmed that our approach to incorporate ceramic beads as drug carrier for highly increased drug load in freeze-gelated matrix scaffolds is feasible and may lead to a sustained drug release and antibacterial activity.

1. Introduction

Bacteria-associated bone infections (osteomyelitis) are characterized by an acute or chronic inflammatory response and often lead to osseous necrosis, bone loss, vascular thrombosis, and joint destruction [1, 2]. Osteomyelitis can be caused by nosocomial infections or superinfections following musculoskeletal injuries, trauma, nosocomial infection, or by orthopaedic operations, irradiation, or bisphosphonate-related osteonecrosis of the jaw (BRONJ). The infection can also spread outward

from the bone and spread in nearby tissues. The treatment of bacteria-associated bone infections is complex and still considered a major problem in orthopaedics and cranio-maxillo-facial surgery. Bone infections can likely lead to implant failure, mortality, and thus associated with a high economic cost [3–6].

Traditional treatments often include surgical debridement, the removal of the injured tissues, and systemic intravenous antibiotic therapy [1,2]. A systemic administration requires large doses of antibiotics for long periods but remains often unsuccessful because many antibiotics have short half-life and can poorly penetrate in the tissues [3]. The limited blood circulation in the infected area implies that only a fraction of the administered antibiotic dose reaches the target site [4,5,7]. Additionally, prolonged or high dose systemic antibiotic administration presents serious side-effects such e.g. systemic toxicity [8,9]. An inappropriate or delayed infection treatment can also induce an antibiotic resistance and biofilm formation at the implantation site. This in turn leads to a formation of a devascularized surface that protects bacteria from antibiotics and makes their usage counterproductive [10–13].

* Corresponding author at: PETROCERAMICS SPA - Kilometro Rosso Science & Technology Park, Viale Europa, 2 - 24040 Stezzano (BG) Italy.

E-mail addresses: uhess@uni-bremen.de (U. Hess), gerd.mikolajczyk1@tu-dresden.de (G. Mikolajczyk), treccanilaura@gmail.com (L. Treccani), philipp.streckbein@uniklinikum-giessen.de (P. Streckbein), christian.heiss@chiru.med.uni-giessen.de (C. Heiss), stefan.odenbach@tu-dresden.de (S. Odenbach), krezwan@uni-bremen.de (K. Rezwan).

¹ Present address: PETROCERAMICS SPA - Kilometro Rosso Science & Technology Park, Viale Europa, 2 - 24040 Stezzano (BG) Italy

An alternative strategy to systemic treatment involves the localized delivery of antibiotics from carrier materials. Insertion of antibiotic containing carriers directly at the site of infection provides higher local antibiotic concentrations than by parenteral administration, and may reduce the risk of systemic toxicity and side effects by lowered systemic concentrations [14–17]. Currently, the clinical standard and most widely employed carrier material consist of poly(methyl methacrylate) (PMMA) in the form of beads or self-setting PMMA bone cements [18–20]. Numerous studies have proven that antibiotic-impregnated PMMA can be efficiently applied for the treatment and prophylaxis of osseous infections [21,22]. However, PMMA is not resorbable and must be removed in a second surgical procedure and the risk of reinfection and increasing patient morbidity are very likely [23,24]. Retention of antibiotic within PMMA is inevitable and only a small percentage of drug is delivered during the functional period of the PMMA implant [25]. Moreover, the monomers required for PMMA polymerization can induce systemic toxicity and the exothermic polymerization reaction can deactivate heat-sensitive antibiotics [26,27].

Alternative carrier materials are biodegradable materials like calcium sulfate and calcium phosphate which are used as resorbable drug delivery systems [14,28–31]. Both materials are resorbable and thus their removal after implantation is not required [31–33], but they feature some drawbacks as e.g. very high resorption rate, quick drug release, and low mechanical strength [26,31,34,35].

In our previous work [36] we show that biodegradable, open porous hydroxyapatite scaffolds can be used as antibiotic depot and release system. Such scaffolds are fabricated using a freeze gelation-based process and antibiotics can be incorporated in the scaffolds in a one-step process without denaturation. However, in these scaffolds only a limited amount of antibiotics can be incorporated as high antibiotic concentrations increase suspension viscosity and scaffold fabrication is hampered.

In this study we present an alternative, versatile route that permits the fabrication of customizable, resorbable open porous calcium phosphate scaffolds with a high drug loading capacity as well as well-controlled, prolonged release. For a targeted release with high drug loading capacity hydroxyapatite and β -tricalcium phosphate beads obtained by ionotropic gelation were loaded with vancomycin and incorporated in an open porous hydroxyapatite matrix scaffold fabricated via freeze gelation. Hydroxyapatite and β -tricalcium phosphate were used due to similar composition to bone and due to their slower resorption and release properties than calcium sulfates [14,15,37].

Vancomycin, a relatively large glycopeptide (MW 1450 Da) and one of the most commonly used drugs for the treatment of infections induced by gram-positive bacteria such as staphylococci and streptococci [38–43] was used as model antibiotic. Vancomycin loading capacity and release were evaluated spectrometrically at 280 nm. The antibacterial activity of the eluents was tested on gram-positive bacterium *Bacillus subtilis*.

Bead loaded scaffolds are envisaged as open porous bone substitute which can be directly inserted in bone cavities or defects. We hypothesised that by embedding antibiotic loaded beads in a porous ceramic matrix antibiotic migration through tissue is prevented and a higher drug concentration at the implantation site can be achieved. The influence of bead incorporation in the scaffold on antibiotic release was assessed likewise spectrometrically.

So far, usually calcium phosphate or calcium sulfate drug carrier can be loaded with drugs either directly during sample preparation, where the drug is mixed with the ceramic [26,28,29,33,35], or the sample is impregnated with the drug afterwards [30,31]. To further enhance the drug loading capacity and to extend drug release even over long time periods, both methods were combined in this study to design multi-loaded beads/matrix composites.

2. Materials and methods

2.1. Materials

Hydroxyapatite (HAP, lot. A3420, specific surface area of 65 m²/g) powder, β -tricalcium phosphate (TCP, lot. BCBB7609, specific surface area of 1.1 m²/g) powder, anhydrous citric acid (lot. BCBB7128), concentrated ammonium hydroxide solution (lot. SZBA1400, $\geq 25\%$), tris(hydroxymethyl)aminomethane (Tris, lot. MKBD9221V), and agar (lot. 050M0202V, ash 2.0–4.5%) were purchased from Sigma Aldrich (Germany). Calcium chloride dihydrate (lot. BCBK7809V) and hydrochloric acid solution (lot. SZBB2900V, 1 M) were obtained from Fluka (Germany) and tri-sodium citrate dihydrate (lot. 3Z003926) and Mueller-Hinton broth (lot. 2W000933) from AppliChem (Germany). Sodium alginate (lot. 90008361, viscosity of 350–550 mPas (1%; 20 °C), pH of 5.5–8.0 (1%; H₂O), BioChemica, Germany), ammonia stabilised silica sol with a SiO₂ content of 30% (lot. 0590b, particle size of 5–8 nm, surface area of 230–360 m²/g, BINDZIL® 30NH3/220, Eka Chemicals, Germany), vancomycin (lot. 172186178, ≥ 900 I.U./mg, Carl Roth, Germany), ethanol abs. (lot. 15B130503, $\geq 99.8\%$, VWR, France) and the gram-positive bacterium *Bacillus subtilis* (*B. subtilis*, DMS cat. no. 1088, Deutsche Sammlung von Mikroorganismen und Zellkulturen GmbH, DSMZ, Germany) were purchased from different suppliers as indicated. Double deionised water (ddH₂O) with a conductivity of 0.05 μ S/cm obtained from an ultra-pure water system (Synergy System, Millipore, Germany) was used for all studies. All chemicals were utilised as received without further purification.

2.2. Bead preparation

HAP or TCP beads were prepared via droplet extrusion coupled with ionotropic gelation in the presence of calcium ions as described by Klein et al. [44]. Briefly, a ceramic/alginate suspension was prepared by adding the HAP or TCP (15.4 wt.%) stepwise to a water-based suspension containing 0.7 wt.% sodium alginate, 0.2 wt.% sodium citrate and 30.3 wt.% silica sol (Fig. 1A). The suspension was evenly stirred (Dispermat LC-2, VMA-Getzmann, Germany; rotating speed: 1000 r/min) and homogenized for 15 min with an ultrasound horn (Sonifier 450, Branson, Germany; power: 150 W, pulse rate: 0.5 s) to remove possible agglomerates. Subsequently, the ceramic/alginate suspension was dropped with a syringe (5 ml Injekt® Luer Solo; needle diameter: 0.55 mm) in a cross-linking solution consisting of ddH₂O, ethanol (ddH₂O/ethanol ratio: 80/20 v/v) and 0.1 mol/l calcium chloride. Beads were left in the cross-linking solution for 18 h. Afterwards they were washed three times with ddH₂O to remove calcium ions in excess. The beads were shortly frozen for 15 min at -150 °C (Ultra-Low Temperature Freezer MDF-1155, Sanyo Electric Biomedical, Japan) and subsequently freeze dried at -20 °C (P8K-E-80-4 -80 °C, Piatkowski, Germany). Part of the beads was rapidly sintered in a tube furnace (VTF1, Vecstar, United Kingdom) for 5 min at two different temperatures, namely 800 °C and 1200 °C. Beads sintered at 800 °C or at 1200 °C are labelled with the suffix: -800 (-1200), respectively (Table 1). Part of the beads was not sintered (suffix: -ns).

2.3. Drug loading

Concentrated vancomycin solutions with three different initial concentrations (1 mg/ml, 10 mg/ml and 100 mg/ml) were used to load $-ns$ or -800 beads. Due to their small surface size, beads sintered at 1200 °C were not further considered. 1 ml vancomycin solution was mixed with 0.11 g beads and incubated at 37 °C under continuous shaking at 100 r/min (Unimax 1010 with Inkubator 1000, Heidolph Instruments, Germany) to guarantee a homogenous drug load. After 15 min the supernatants were removed. Preliminary kinetic drug loading measurements indicated that the largest vancomycin percentage was loaded in the first 5 to 10 min (see supporting data: Fig. B.1 in the online version at

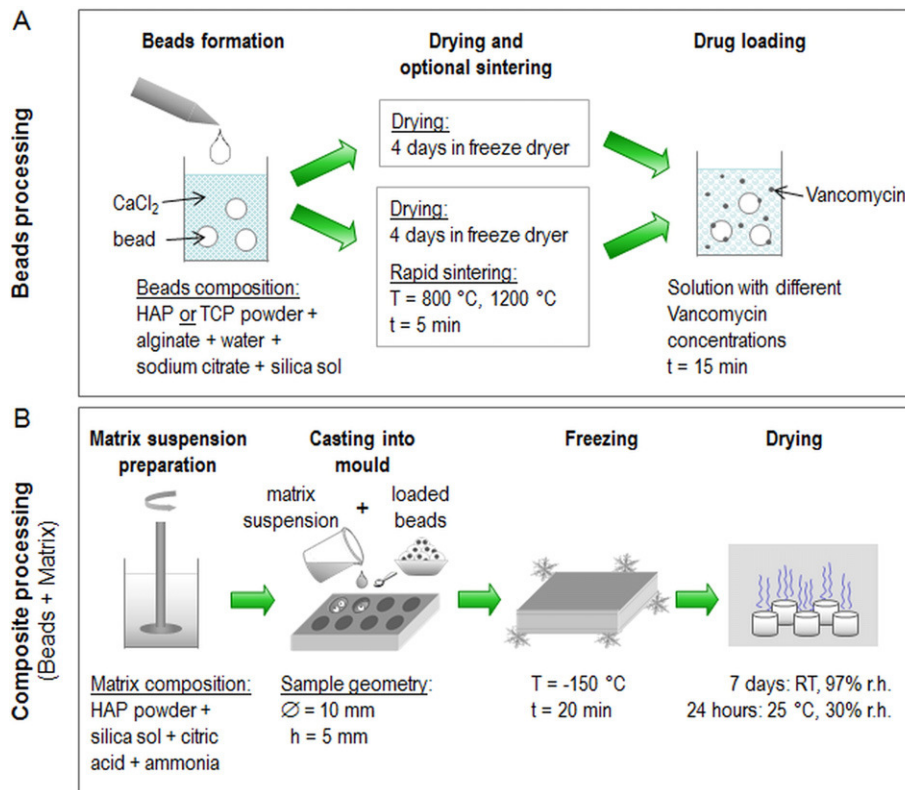


Fig. 1. A: Schematic overview of the manufacturing process of hydroxyapatite (HAP) or β -tricalcium phosphate (TCP) beads by ionotropic gelation. **B:** Composite preparation by incorporation of beads in an open-porous scaffold matrix by freeze gelation process.

<http://dx.doi.org/10.1016/j.msec.2016.05.042>). The quantity of loaded antibiotics was calculated via depletion method. Vancomycin concentrations were spectrometrically measured at 280 nm using a microplate spectrophotometer (Multiskan GO, Thermo Scientific, Finland). Prior to these measurements, the supernatants were centrifuged for 15 min at 14,500 r/min (Heraeus Fresco 21, Thermo Scientific, Germany) to separate and remove any particulates possibly disturbing the measurement. Measurements were done in triplicates and all samples were used in quadruplicates.

2.4. Composite preparation

Beads/matrix composites were obtained by incorporating vancomycin loaded HAP or TCP beads (–ns and –800, respectively) in open-porous HAP scaffolds (matrix) obtained by freeze gelation and described in our previous studies [36,45]. In short, the matrix was obtained using a water-based HAP suspension (59.34 wt.%) with 1.98 wt.% silica sol as gelling agent and 1.93 wt.% citric acid as dispersant agent was continuously stirred at 1500 r/min (Fig. 1B). Ammonia solution was added to adjust the pH to 8.

Vancomycin loaded beads were first homogeneously mixed with the HAP suspension (beads/suspension ratio: ~1/11.5 w/w) and then poured in cylindrical polyvinyl chloride (PVC) moulds of 10 mm diameter and 5 mm height. After filling, the moulds were frozen for 20 min at –150 °C. The demoulded samples were dried at room temperature and

a relative humidity (r.h.) of ~97% for 7 days in a desiccator and finally dried another day at 25 °C and 30% r.h.

2.5. Bead and composite characterization

Bead density was measured by helium-pycnometrie (Pycomatic ATC, Thermo Scientific, Italy). Specific surface area (S_{BET}) as well as bead pore volume were determined by nitrogen adsorption (Belsorp-Mini, Bel, Japan) using the Brunauer-Emmett-Teller (BET) method [46]. Bead open porosity and pore sizes were measured via mercury-intrusion porosimetry (Pascal 140/440, Porotec, Germany). Contact angle and surface tension of mercury were assumed to be 141.3° and 480 mN/m, respectively. Beads and scaffolds were imaged via scanning electron microscopy (SEM, acceleration voltage 20 kV, CamScan, UK). X-ray micro-computed tomography (μ -CT) of a matrix scaffold with beads was performed using a nano focus tube (XS160NFOF, GE Sensing and Inspection Technologies, Germany) with a tungsten target, an acceleration voltage of 90 kV and a cathode current of 170 μ A. The attenuated X-rays were captured using a detector (Shad-o-Box 4K EV, Rad-Icon Imaging Corporation, USA) with a resolution of 2048 \times 2000 pixel, an according pixel pitch of 48 μ m and a digitization of 12 bit. Radiographs were taken with an angular increment of 0.25° over a full rotation of 360°. The magnification due to the cone beam was 9. Reconstruction was based on a FDK-algorithm and the resulting pixel pitch of the reconstructed tomogram was ~11 μ m.

Bead degradation behaviour was assessed by measuring the calcium (Ca^{2+}) ion release. 0.3 g beads were soaked in 1.5 ml Tris-HCl buffer (pH 7.4) and the samples were continuously shaken at 100 r/min in an incubator (Unimax 1010 with Inkubator 1000, Heidolph Instruments, Germany) at a constant temperature of 37 °C. The solutions were changed every 24 h up to 14 days and the Ca^{2+} content in the supernatants was measured. Prior to measurement, the supernatants were centrifuged for 15 min at 14,500 r/min (Heraeus Fresco 21, Thermo Scientific, Germany) to separate and remove any particulates.

Table 1
Suffix nomenclature.

Suffix label	Explanation
-ns	Beads were not sintered
-800	Beads were sintered at 800 °C
-1200	Beads were sintered at 1200 °C

Ca²⁺ concentration was measured photometrically at 578 nm (XION 500, Dr. Lange, Germany) using a calcium-o-cresolphthalein-based colorimetric assay (Fluitest CA CPC, Analyticon Biotechnologies, Germany). Measurements were done in triplicates and all samples were used in quadruplicates.

2.6. Drug release

Antibiotic release from 0.11 g vancomycin loaded beads was measured daily for 5 days under continuous shaking at 100 r/min and 37 °C. 1.5 ml Tris-HCl buffer (0.1 mol/l) with an initial pH of 7.4 at 37 °C was used and replaced every 24 h. As reference non-loaded beads were used and treated in the same way. The amount of released vancomycin was directly measured at 280 nm (λ_{max}) via UV/VIS spectroscopy. Vancomycin release from cylindrical HAP-matrix scaffolds (diameter: 9.1 mm \pm 0.1 mm; height: 4.8 mm \pm 0.3 mm; weight: 0.4 g \pm 0.1 g) containing 0.11 g loaded beads was determined as previously described. For each cylindrical HAP-matrix scaffold 2 ml Tris-HCl buffer was used.

2.7. Antibacterial activity

The antibacterial activity of released vancomycin was determined using a standard inhibition test method with agar plates [47]. Gram-positive bacterium *B. subtilis* was precultured in Mueller-Hinton broth at 37 °C overnight. Then 200 μ l of bacteria solution with a concentration of 2×10^8 cells/ml, which was determined in accordance to McFarland standards [48], was spread uniformly with a Drigalski spatula on Mueller-Hinton agar plates (1.7 wt.% agar). Cotton platelets ($\varnothing = 9$ mm, Rotilabo®-test flakes, Carl Roth, Germany) were placed on the inoculated agar plates and loaded with 60 μ l of the eluents of the release test. Finally, the antibacterial effect was determined by measuring the zones of inhibition (ZOIs) formed around the cotton platelets.

2.8. Multi-loaded composites

To obtain multi-loaded composites three different loading methods were used as shortly summarised in the following table (Table 2).

By using these three drug loading methods four different sample types were produced (schematically shown in Fig. 9A) and compared:

- 1) Sample I: Unloaded HAP matrix scaffolds with vancomycin loaded beads
- 2) Sample II: Vancomycin loaded HAP matrix scaffolds with vancomycin loaded beads
- 3) Sample III: Unloaded HAP matrix scaffolds with vancomycin loaded beads soaked in vancomycin solution
- 4) Sample IV: Vancomycin loaded HAP matrix scaffolds containing vancomycin loaded beads soaked in vancomycin solution

Total incorporated vancomycin amount for each method and sample type was measured and calculated as described in Section 2.3. Vancomycin release and antibacterial activity assessment were carried out as described in Sections 2.6 and 2.7. For release experiments 200 μ l of supernatants was removed after 1, 2, 4, 8, 12, 24, 32, 48, 54, 72, 96

Table 2
Different vancomycin loading methods.

Method	Procedure
Method 1	T-ns beads were loaded by soaking as described in Section 2.3
Method 2	Vancomycin (1 wt.%) was incorporated in the HAP matrix suspension prior to unloaded bead addition and using the procedure described in [36]
Method 3	Vancomycin unloaded beads/matrix composites were soaked in 0.5 ml concentrated vancomycin solution (100 mg/ml) for 5 min

and 120 h and used for drug quantification and antibacterial tests. Removed supernatants were replaced with 200 μ l fresh Tris-HCl.

3. Results

3.1. Bead characterization

Bead properties before and after sintering are summarised in Table 3. In general bead properties depend on the ceramic powder used and on the sintering temperature applied.

Non-sintered HAP beads featured a density of 2.29 ± 0.0004 g/cm³, a diameter of 1.05 ± 0.13 mm, a specific surface area (S_{BET}) of 90.5 ± 1.2 m²/g, an open porosity of 63.4%, a pore volume of 68.4 ± 0.3 mm³/g, and a bimodal pore size distribution (see supporting data: Fig. A.1 in the online version at <http://dx.doi.org/10.1016/j.msec.2016.05.042>.) with average pore diameters of 35 nm and 476 nm, respectively. After sintering of HAP beads at 800 °C, density increased 18% and shrank 10%. S_{BET} was reduced by 42 m²/g and pore volume was decreased to 31.6 ± 6.1 mm³/g. Open porosity increased by sintering of 800 °C about 14%. HAP-800 beads featured also a bimodal pore size distribution with increased pore diameters to average 59 nm and 476 nm. After sintering up to 1200 °C, density increased 19% and shrank 38%, compared to non-sintered HAP beads. S_{BET} was reduced considerably by 89 m²/g to 1.2 ± 0.3 m²/g, open porosity was reduced by 38% to 23%, and pore volume was decreased by 68 mm³/g to 0.8 ± 0.1 mm³/g. HAP beads sintered at 1200 °C featured a monomodal pore size distribution with an average pore diameter of 764 nm.

Non-sintered TCP beads showed a density of 2.54 ± 0.0009 g/cm³, a diameter of 1.20 ± 0.18 mm, a S_{BET} of 55.8 ± 0.4 m²/g, an open porosity of 48.2%, a pore volume of 45.5 ± 6.3 mm³/g, and a bimodal pore size distribution with average pore diameters of 19 nm and 121 nm, respectively. After sintering of TCP beads at 800 °C, density slightly increased about 4% and S_{BET} slightly decreased 5 m²/g. Bead diameter shrank 16% to 1.20 ± 0.18 mm. Open porosity of TCP beads increased by sintering 800 °C about 11%, and pore volume decreased 12 mm³/g. Pore size distribution was bimodal with average pore diameters of 29 nm and 144 nm, respectively. By sintering 1200 °C, TCP beads shrank about 32% and density increased slightly 6%, compared to non-sintered beads. The reduction in S_{BET} of TCP-1200 beads was 39 m²/g. Open porosity decreased 32%. Pore volume decreased 34 mm³/g to 11.6 ± 3.5 mm³/g. Pore diameters with a bimodal pore size distribution increased to around 37 nm and 150 nm, respectively.

Surface morphology and geometry differed between HAP and TCP beads and were particularly influenced by the sintering temperature applied (Fig. 2). The surface of non-sintered HAP beads was smooth, uniform, and they featured nearly spherical form. With increasing sintering temperature HAP beads shrank and became ellipsoidal and the surface was more roughed. In contrast, TCP beads were more structured and had an angular and wrinkled surface already in the non-sintered stage. Cross sections showed that non-sintered beads had a shell like structure. This is even more pronounced for non-sintered TCP beads. All sintered beads had a more homogeneous inner structure and fewer pores were visible compared to non-sintered beads for both materials.

The degradation behaviour of the ceramic beads at pH 7.4 was determined by measuring the calcium ion (Ca²⁺) release as a function of time over two weeks. All samples showed an increasing, time-dependent Ca²⁺ release (Fig. 3). TCP-ns (12.04 ± 0.61 mmol/l), TCP-800 (13.4 ± 0.52 mmol/l) and HAP-800 (11.87 ± 0.39 mmol/l) showed a higher cumulative Ca²⁺ release after 14 days compared to TCP-1200 (4.85 ± 0.58 mmol/l), HAP-ns (4.45 ± 0.41 mmol/l), and HAP-1200 (2.26 ± 0.21 mmol/l). HAP-800 and TCP-1200 showed a linear release. All other samples (HAP-ns, HAP-1200, TCP-ns, TCP-800) showed an initial burst release followed by a reduced release. The same quantity of cumulated released Ca²⁺ ions presented TCP-1200 and HAP-ns after 13 days, and TCP-ns and HAP-800 after 14 days, respectively.

Table 3

Properties of HAP and TCP beads non-sintered (–ns) and sintered at 800 °C (–800) and 1200 °C (–1200) for 5 min.

Bead type	Density (g/cm ³) [†]	Diameter (mm) [§]	Specific surface area, S _{BET} (m ² /g) [‡]	Open porosity (%) ^{§,a}	Pore volume (mm ³ /g) [‡]	Average pore diameter (nm) ^{§,a}	Pore size distribution [§]
HAP-ns	2.29 ± 0.0	1.05 ± 0.13	90.5 ± 1.2	63.4	68.4 ± 0.3	35/476	Bimodal
HAP-800	2.71 ± 0.0	0.95 ± 0.22	48.1 ± 0.2	72.4	31.6 ± 6.1	59/651	Bimodal
HAP-1200	2.72 ± 0.0	0.65 ± 0.09	1.2 ± 0.3	23.0	0.8 ± 0.1	764	Monomodal
TCP-ns	2.54 ± 0.0	1.20 ± 0.18	55.8 ± 0.4	48.2	45.5 ± 6.3	19/121	Bimodal
TCP-800	2.65 ± 0.0	1.01 ± 0.13	50.5 ± 2.5	53.6	33.8 ± 7.6	29/144	Bimodal
TCP-1200	2.69 ± 0.0	0.82 ± 0.14	17.0 ± 3.2	32.8	11.6 ± 3.5	37/150	Bimodal

Measured by: He-pycnometry[†], geometrical measurement[§], N₂-adsorption[‡], Hg-intrusion[§].^a Single measurement.

3.2. Bead drug loading

Preliminary measurements of kinetic drug loading indicated that after 15 min the initial drug load has been completed, irrespective of the bead material or the initial concentration of the antibiotic solution (see supporting data: Fig. B.1 in the online version at <http://dx.doi.org/10.1016/j.msec.2016.05.042>). HAP and TCP beads showed a similar vancomycin uptake behaviour and only a considerable difference was observed at the highest vancomycin concentration applied (100 mg/ml) (Fig. 4). At this concentration non-sintered HAP and TCP beads were able to load ~55 mg/g more than sintered beads.

3.3. Bead drug release

Independent of the bead type or the initial vancomycin concentration used for loading, all samples showed maximum absolute drug release at day 1 (Fig. 5A and B). For Vancomycin solution with an initial concentration of 10 mg/ml between 33.6 ± 0.50 mg/g (TCP-ns) and

45.6 ± 1.02 mg/g (TCP-800) was released at day 1 (Fig. 5A). The amount of released vancomycin for HAP beads was in between. After day 3 almost no drug was further released. For vancomycin solution with an initial concentration of 100 mg/ml the released drug quantity was considerably higher and the period where released vancomycin was still measurable was prolonged (Fig. 5B). At least at day 4 vancomycin can still be measured in the supernatants. The highest release was measured at day 1 between 89.7 ± 5.62 mg/g (TCP-ns) and 97.6 ± 5.05 mg/g (HAP-800). Only non-sintered HAP beads had a higher vancomycin release of 165.2 ± 11.56 mg/g.

For initial concentration of 10 mg/ml, an increased cumulative percentage vancomycin release within the first two days was determined (Fig. 5C). For a higher solution concentration of 100 mg/ml this period could be prolonged up to day 3 to 4 (Fig. 5D). Whereas at 800 °C sintered TCP beads loaded with 10 mg/ml vancomycin reached a cumulative drug release of ~100% after 5 days, and non-sintered TCP beads only released three-quarters of the loaded drug quantity. Also for 100 mg/ml vancomycin solution the highest percentage of loaded drug was

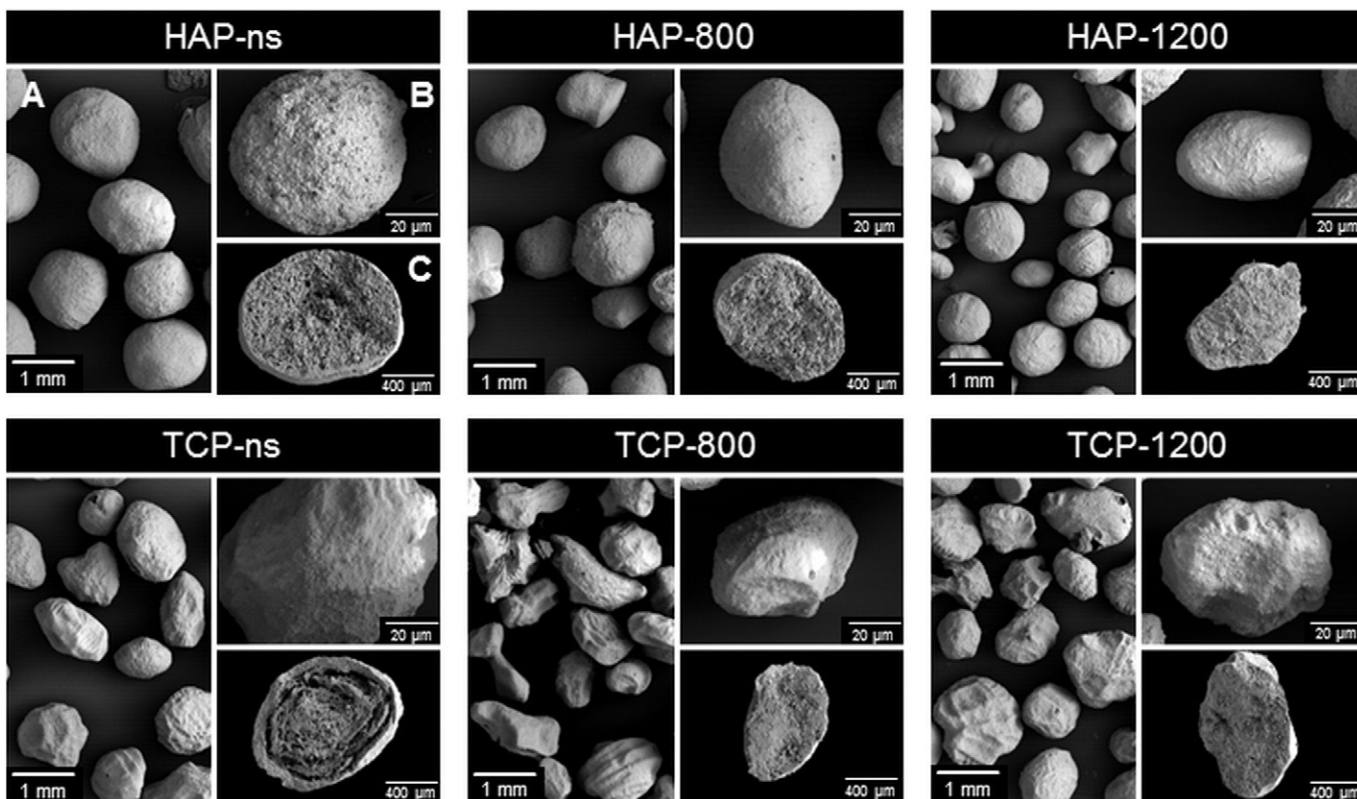


Fig. 2. Surface morphology and geometry of HAP and TCP beads non-sintered and sintered at 800 °C and 1200 °C. Representative SEM images of bead geometry (A), bead surface (B) and cross section (C).

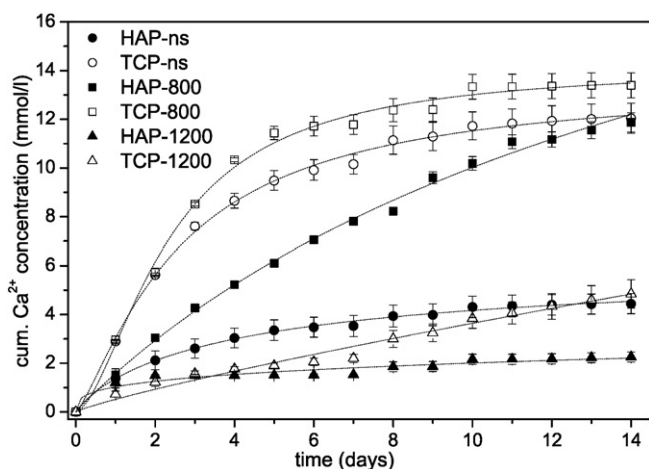


Fig. 3. Degradation behaviour of non-sintered and sintered beads in Tris-HCl buffer at pH 7.4 and 37 °C. The concentration of released Ca^{2+} up to 14 days was measured by a colorimetric assay via UV/VIS spectroscopy. The buffer was exchanged daily.

released by TCP beads sintered at 800 °C ($93.7 \pm 8.61\%$) and the lowest for non-sintered TCP beads ($64.3 \pm 2.17\%$). In both cases HAP beads had a percentage drug release in between.

3.4. Composite drug release

Vancomycin loaded beads were successfully incorporated in open porous, near-net-shaped HAP matrix scaffolds obtained by freeze gelation. After bead incorporation, scaffolds featured a good initial stability and could be easily handled without any deterioration.

For this study, only small cylinders were used (Fig. 6A, b and B), but other and more complex geometries can be obtained as demonstrated by the exemplary photograph showing a geometrical copy of a part of the lower jaw from an adult domestic pig (Fig. 6A, a). For both samples it is valid that from the outside, the embedded beads cannot be identified. They are completely covered by the scaffold matrix. Cross section of a μ -CT image shows the matrix scaffold in a cylindrical sample used in this study (Fig. 6B). The visible spherical cavities represent the hidden beads. As trend, more cavities and therefore beads are visible in the upper part of the composite. Micrograph illustrates open porous beads (additionally highlighted by green colour) embedded in open porous scaffold matrix (Fig. 6C). The beads are closely packed together but not in contact. It appears that the outer shell of the beads is denser as the porous interior, as could already be seen more clearly in Fig. 2.

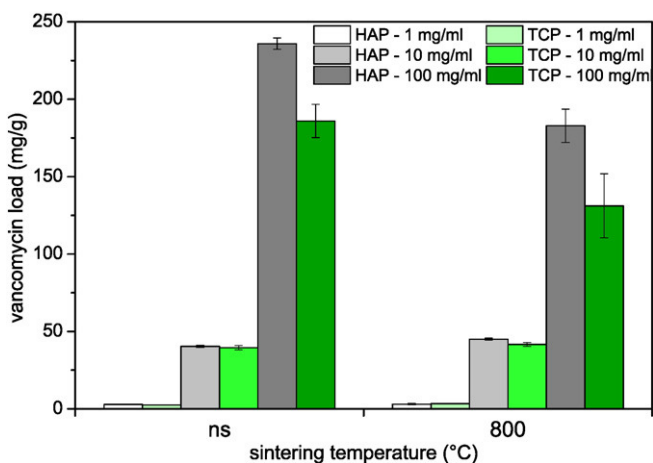


Fig. 4. Loaded vancomycin amount (in mg per g beads) of non-sintered (ns) and at 800 °C (800) sintered HAP and TCP beads. Beads were loaded with vancomycin concentrations of 1, 10 and 100 mg/ml.

Vancomycin release profile was similar in beads/matrix composites as compared to only beads (Fig. 7). Incorporated beads prior loaded with 10 mg/ml vancomycin showed drug release up to day 3 with a maximum release after day 1 (~ 50 mg/g). For beads loaded with 100 mg/ml, the release period was prolonged up to day 5. The maximum release after day 1 varied between 107.5 ± 2.63 mg/g (TCP-ns) and 185.0 ± 7.21 mg/g (HAP-ns). $79.4 \pm 7.29\%$ of the loaded vancomycin was released after 5 days from composites with non-sintered HAP beads loaded with 10 mg/ml. For sintered TCP beads the release was $100.9 \pm 3.90\%$. For composites with incorporated beads loaded with 100 mg/ml the release varied between $71.5 \pm 0.04\%$ (TCP-ns) and $101.9 \pm 1.03\%$ (TCP-800).

3.5. Antibacterial activity

Inhibition zone test with the eluents of release test on gram-positive *B. subtilis* indicated an antibacterial activity of the released vancomycin (Fig. 8). A clear visible inhibition zone (ZOI) formed around the cotton platelets. ZOIs were reduced at each new time point. For beads loaded with 10 mg/ml vancomycin and incorporated or non-incorporated in matrix scaffold, an antibacterial effect could be measured up to day 3. For beads loaded with 100 mg/ml the antibacterial effect could be prolonged compared to lower vancomycin concentration, besides for TCP-800 beads. For incorporated HAP beads, antibacterial effects up to day 5 were observable.

3.6. Multi-loaded composites

To prolong the antibacterial effect of released vancomycin and to increase the loadable drug quantity different, multi-loaded beads/matrix composites were applied (Fig. 9A). It was possible to increase the loaded vancomycin quantity, as compared to composites with only loaded beads (Sample I), by also loading the matrix while sample preparation by directly adding vancomycin to the matrix suspension (Sample II) (Fig. 9B). A comparable drug quantity could be achieved by post-impregnation of the composites (Sample III). By combining all three methods, a maximum drug loading of ~ 37 mg per sample could be realized (Sample IV).

Looking at more measurement time points in the vancomycin release, especially in the beginning, then a more detailed view of the drug release could be observed (Fig. 9C). In the first hours of elution of the composites, still a burst release was observed. No later than 2 days, merely smaller amounts of drug were released. In between, in all samples a more or less pronounced stepwise release behaviour was shown. Composites wherein only beads were loaded had a release of $49.5 \pm 2.18\%$ up to 12 h. Up to about 32 h, little vancomycin was further released. Then a stronger release of 17.2% during the next 16 h could be observed. Subsequently, only little drug was delivered to the end of the investigation period again. If the matrix was also loaded with vancomycin, 4.8% less was released in total compared to composites with only loaded beads within the 5 days. Up to 8 h after the start of the elution $39.0 \pm 2.45\%$ (Sample II) was released. Between 8 h and 24 h, only a little ($\sim 1.7\%$) was released before a further burst release of 20.7% occurred between 24 and 32 h. Most of the loaded drug was released from composites with loaded beads which were also infiltrated ($84.4 \pm 2.01\%$). There was a burst release of $64.1 \pm 2.40\%$ within the first 4 h. After that, an average of around 0.3%/h was released. This release rate was further decreased after around 54 h. In composites with loaded beads as well as matrix, which were also infiltrated, after 5 days $77.1 \pm 0.68\%$ was released. Within the first 4 h $45.5 \pm 2.78\%$ was released. Again, in the next 50 h 29.1% was released. After that, there was only a small release.

In contrast to the other composites, scaffolds with only loaded beads showed no ZOI at day 5 (Fig. 9D). The highest antibacterial effect could be achieved for scaffolds with loaded beads, loaded matrix, and post-soaking.

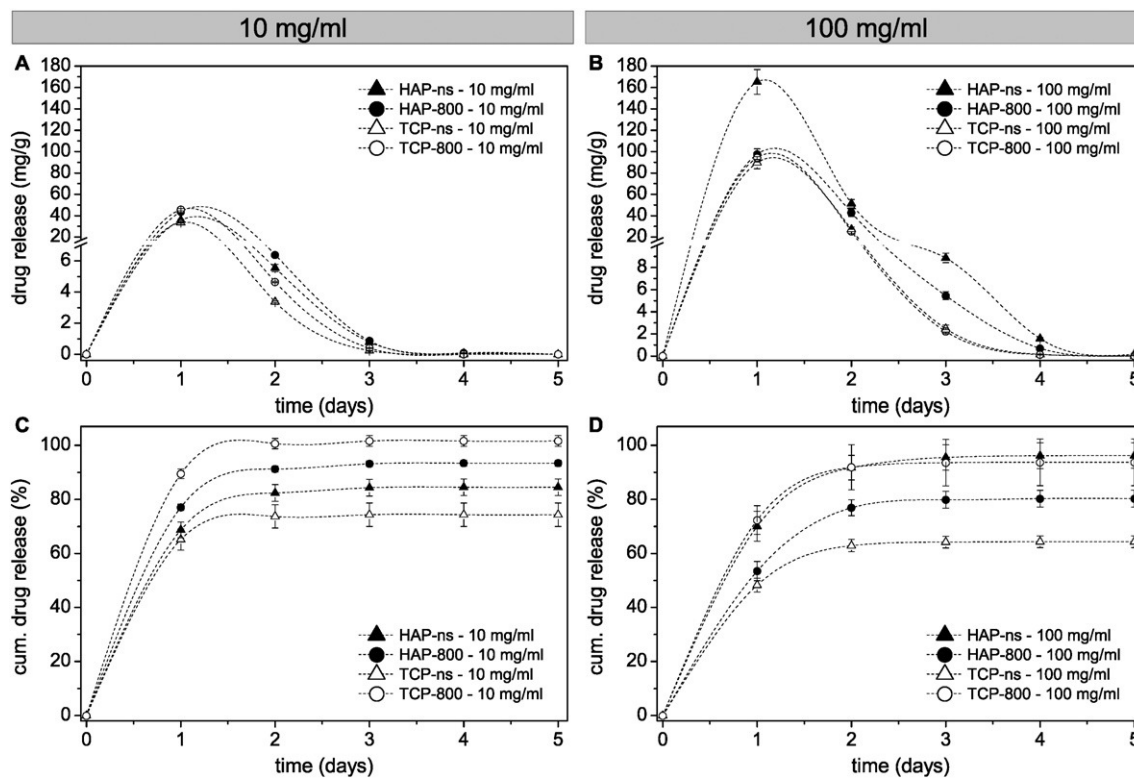


Fig. 5. Absolute (A, B) and cumulative percentage (C, D) vancomycin release from non-sintered and at 800 °C sintered beads over 5 days. The amount of released vancomycin was determined by UV/VIS spectroscopy at 280 nm. The samples were stored at 37 °C in a Tris-HCl buffer with pH 7.4. The beads were loaded with an initial vancomycin concentration of 10 mg/ml (A, C) and 100 mg/ml (B, D) for 15 min.

4. Discussion

Calcium phosphate beads/matrix composites could be successfully prepared by freeze gelation. It could be shown that they might be suitable as scaffolds with an antibacterial activity due to the release of active vancomycin.

As part of this work, beads were successfully prepared with different calcium phosphates by droplet extrusion coupled with ionotropic gelation. The ionotropic gelation of natural polysaccharides like alginate with ceramic particles is an established method to produce ceramic beads with tuneable properties [44,49,50]. In this study we could show that bead characteristics, such as morphology, specific surface area (S_{BET}), pore size, and pore size distribution, depend mainly on calcium phosphate type and sintering temperature used. By sintering the alginate is burned out resulting in pure ceramic beads, and pore size and stability are increased. On the other hand, sintering leads to a significant reduction of the S_{BET} , the open porosity and pore volume with

concomitant bead shrinkage. In order to still retain a large S_{BET} , rapid sintering in a tube furnace was used [51]. The S_{BET} can be further increased by the additional use of silica, that might reduce the pore size [44]. However, as the drug size usually used is much smaller than that of the pores, this should not be a hindrance for a homogenous drug loading and distribution. At 1200 °C the contained SiO_2 results to a beginning transformation of HAP to β -TCP [52–54] (for XRD-analysis see supporting data: Fig. C.1 in the online version at <http://dx.doi.org/10.1016/j.msec.2016.05.042>). At lower temperatures or for TCP beads no phase changes or other alterations could be observed by sintering. In comparison to alumina/silica beads [44,51] a distinct multimodal porosity was achieved for all types of beads except HAP-1200. Such meso-porosity is likely to be generated by silica nanoparticles and the alginate network.

The calcium phosphate powder used can also affect bead characteristics. The rougher and less homogenous surface of TCP beads might be related to TCP dissolution [55,56]. Released Ca^{2+} ions from TCP can

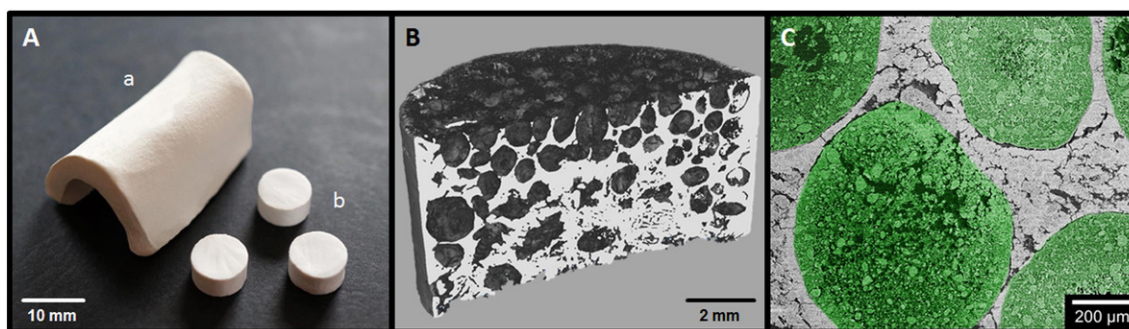


Fig. 6. A: Photo of an exemplary near-net-shaped scaffold representing the geometrical copy of a part of the lower jaw of an adult domestic pig (a) and cylindrical samples used for this study (b). B: μ -CT image of the frontal plane of the matrix from a beads/matrix-composite with hidden HAP-ns beads. C: Micrograph from composite of porous beads (green) incorporated in open porous HAP-scaffold matrix (grey). Open porosity was obtained by ice crystals during composite preparation.

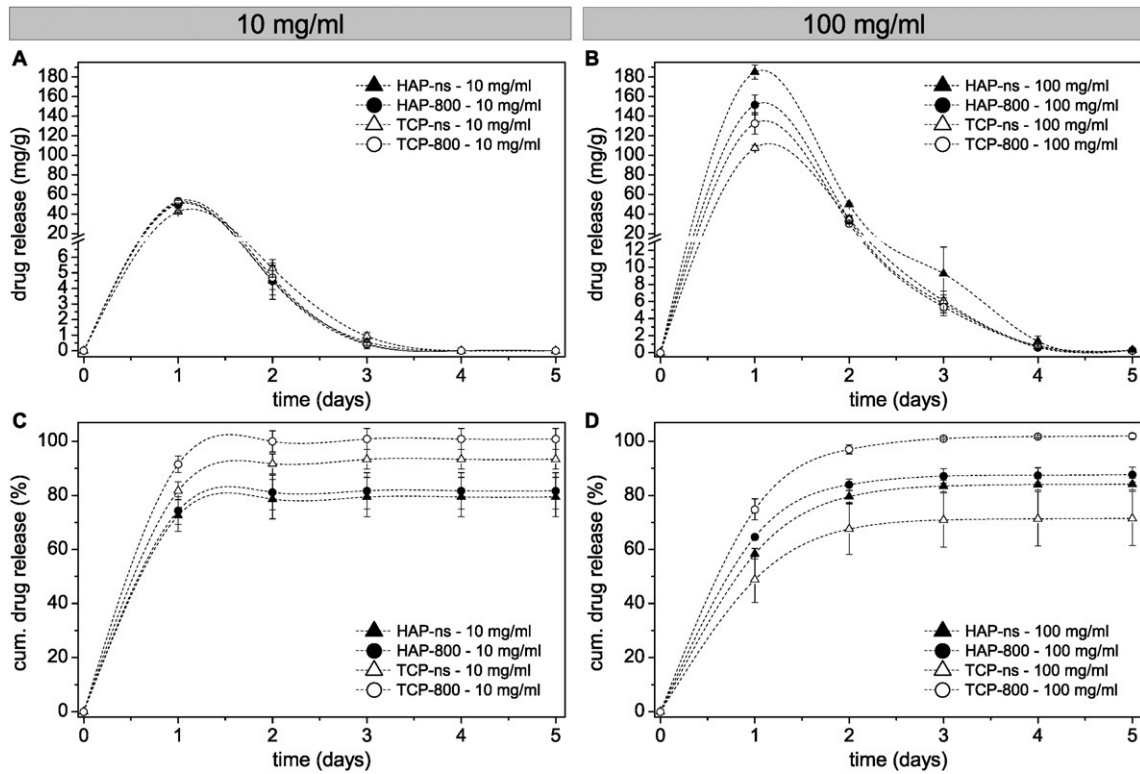


Fig. 7. Absolute (A, B) and cumulative percentage (C, D) released vancomycin from loaded beads incorporated in HAP-scaffolds over 5 days. The amount of released vancomycin was determined by UV/VIS spectroscopy at 280 nm. The samples were stored at 37 °C in a Tris-HCl buffer with pH 7.4. The beads were loaded with an initial vancomycin concentration of 10 mg/ml (A, C) and 100 mg/ml (B, D).

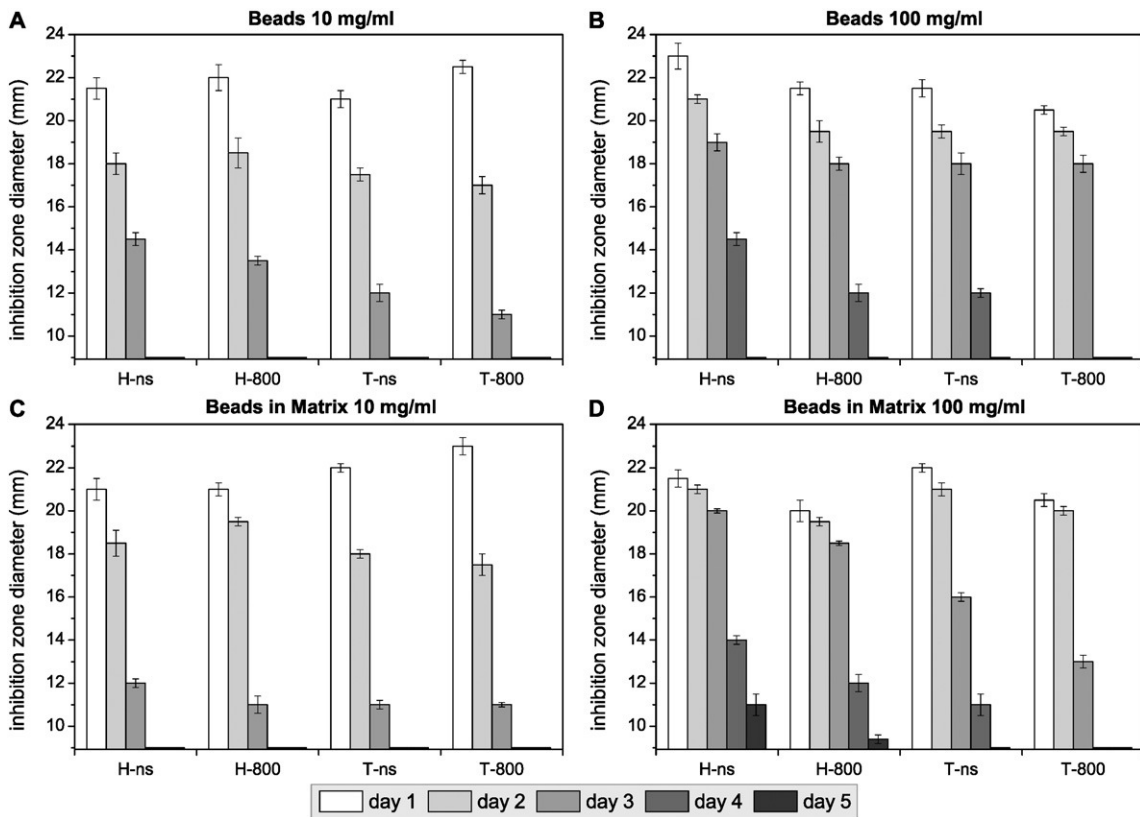


Fig. 8. Assessment of the antibacterial activity of released vancomycin from loaded beads (A, B) and loaded beads incorporated in matrix (C, D) by inhibition zone test. Inhibition zone diameters (in mm) on agar plates as antibacterial effect of released vancomycin on *B. subtilis* are measured. Each platelet with a diameter of 9 mm was seeded with 60 μ l eluent of the release test.

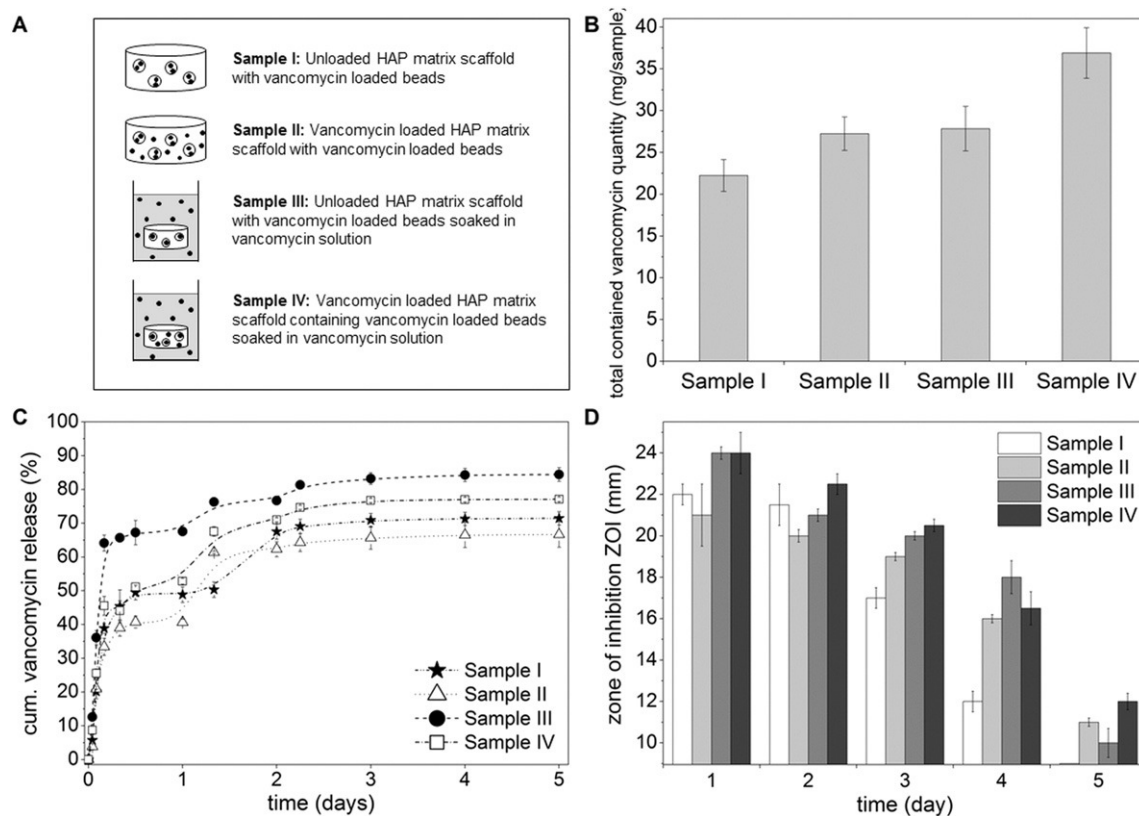


Fig. 9. Multi-loaded beads/matrix composites. All composites contained 0.11 g loaded or non-loaded beads. A: Schematic drawing and explanation of the experimental groups. B: Total loaded vancomycin quantity before release in mg per sample. C: Percentage cumulative vancomycin release (%). D: Assessment of the antibacterial activity of released vancomycin from multi-loaded beads/matrix composites by inhibition zone test. Inhibition zone diameters (in mm) on agar plates as antibacterial effect of released vancomycin on *B. subtilis* are measured. Each platelet with a diameter of 9 mm was seeded with 60 μ l eluent of the release test.

compete with Ca^{2+} present in the linking solution, occupy the binding sites of alginate and thus lead to a faster cross-linking [44,57,58]. The formation of an outer shell at T-ns beads could be related to non-uniform gelation.

The different solubilities of the used powders for bead preparation as well as the sintering temperature are also reflected in the different solubilities of the beads. TCP beads showed a faster degradation than HAP beads. The fastest degradation could be observed for beads sintered at 800 °C since the alginate as stabilising factor is already burned out and the sintering of the ceramic powder did not start yet. Also the high porosity and thus the accessibility played a key role in solubility behaviour [59].

To use the beads as drug carrier, high S_{BET} and tailorable pore volume as well as pore size distribution are required and given here. Since the beads were not washed after loading, a considerable amount of drug was not only bound but also present in the pores. This increased the maximum drug loading amount remarkably, especially for substances with a lower binding affinity to calcium phosphate. Usually, only large surface areas are important for improved drug adsorption behaviour. In the present study also the pore volume was essential resulting in higher drug loading capacities. The high bead open porosity, which is usually accompanied by high pore interconnectivity, can favour liquid penetration, a good ability for drug load. Pore sizes between 19 and 651 nm are large enough for vancomycin uptake (size: $\sim 3.2 \times 2.2$ nm [39]) although it is already one of the rather large drug molecules. However, the large molecule size might be a limiting factor for its loading and complete filling of the pores with a high packing density due to steric hindrance [60]. Also, although it has one carboxylic group, vancomycin often shows only weak interactions with calcium phosphate [60]. In order to obtain a maximum drug loading, mainly the drug concentration must be increased. Beads sintered at 1200 °C were not further

considered due to their small surface size and pore volume and the thus expected low loading capacity. In this study, a loading time of 15 min was chosen because preliminary kinetic measurements showed an increase in drug load up to 5 min (TCP-ns) and 10 min (HAP-ns), respectively (see supporting data: Fig. B.1 in the online version at <http://dx.doi.org/10.1016/j.msec.2016.05.042>). During this period of 15 min, an almost maximum drug load can be assumed while a possible decomposition of the beads in this time is still considered to be negligible.

Advantages of the beads as drug carrier are no use of toxic substances and that high sintering temperatures are not essential even as green body stability and chemical resistance are high enough for handling as well as drug loading and release. No or low sintering temperatures result in enhanced degradation which avoid further surgeries to remove the drug carrier after they are empty and no longer required. HAP beads tend to absorb a little more vancomycin than TCP beads. The larger open porosity, pore volume, and pore diameter allow better accessibility. The advantages and disadvantages of sintering (greater porosity and pore sizes vs. smaller surface area) seem thereby to compensate itself, largely based on the amount of drug absorbed.

Vancomycin loaded beads could be used as drug carrier in a bacterial infected bone cavity with a drug releasing ability. However, for preventing an uncontrolled and undesirable spreading and migration of the drug carrier at the implantation site, the loaded beads were embedded in an open porous, degradable, stable, near-net-shape hydroxyapatite scaffold. The freeze gelation process allows it to produce complex, customized to the patient implant geometries [36,45]. The integration of large particles (beads) in freeze gelled scaffolds was possible without larger cracks which could impair their properties.

Stable beads/matrix scaffolds using the freeze gelation process can only be achieved with ceramic beads. As preliminary investigations have demonstrated (data not shown), a production of scaffolds with

integrated pure alginate beads is not possible. The ceramic content in the beads reduces swelling by dehydration of the matrix suspension and prevents a blasting of the scaffold structure. During drying pure alginate beads shrink again and can fall out of the scaffold matrix. Small amounts of alginate, as they occur in non-sintered beads, seem to have no pronounced negative effect on the structure of beads/matrix composites.

It would have been expected that the beads sink in the matrix suspension and sediment concentrated at the bottom. However, the μ -CT scan (Fig. 6B) shows that the beads tend to concentrate at the sample top. The floating in the matrix suspension (density $\rho = 1.6 \pm 0.33 \text{ g/cm}^3$) results from the large porosity and smaller density of the beads ($\rho = 0.84 \text{ g/cm}^3$ for HAP-n beads in consideration of the open porosity) and the fact that the pores in the interior are not fully infiltrated with suspension (Fig. 6C). Except to the vertical gradient shown in Fig. 6B, the beads are homogeneously distributed in the scaffold. Due to their larger size compared with the matrix suspension particle size and the ice crystal size, the beads are encapsulated by the moving interface while freezing [61,62].

However, due to the open porous matrix structure, it is possible that the beads loaded with active drugs can be flowed through and thus the drugs can be released. Drug release from beads or beads embedded in a matrix is hardly different. The matrix is open porous and the pores are large enough to not create a diffusion barrier. The beads can be almost completely reached and flowed through by the liquid, which makes it as consequence easy to release. Based on the test results, the drug release may be referred as diffusion controlled. Although degradation of matrix and beads takes place, it is considerably slower than the release of the drugs. Using large concentrations (100 mg/ml) of antibiotics in the initial sample, the period of the quantifiable release was extended from 3 days to 4 days irrespective of the bead type. Since not all sides from the individual beads can be completely attained and a part of the drug may adsorb on the pores during diffusion, not the entire amount of loaded vancomycin was completely released during the investigation period for most samples.

This study has demonstrated the ability to integrate effective antibiotics in beads and to produce antibacterial beads/matrix composites. The inhibition test method could prove that all processing steps do not hinder or disturb the antibacterial activity and inhibited bacterial growth. The samples may show a 1 day longer bacteriostatic effect than detectable with the UV/VIS. Accordingly, it is assumed that although photometrically no more drug release was detectable, a sufficient amount of vancomycin was released in order to be above the minimum inhibitory concentration (MIC) of gram-positive *B. subtilis* (MIC: $\sim 0.125\text{--}0.25 \mu\text{g/ml}$ [63,64]). Again, composites with high initial drug concentration showed the longest antibacterial activity.

It has been found that the amount of drug loaded plays an essential role with respect to a prolongation of the release duration and the antibacterial efficacy. To increase the maximum absorbable quantity of antibiotics per sample even further, samples were loaded multiple times. One of our previous studies showed that an incorporation of vancomycin in the scaffold structure via a one-step process is possible [36]. The incorporation of antibiotics into the matrix structure can build a drug depot with the effect that the rest of the embedded drugs releases in a longer period of time while the scaffold is gradually degraded. The release kinetics are no longer majority controlled by diffusion, but also controlled by degradation. To fight a possible infection quickly, already loaded beads/matrix composites can be additionally soaked in an antibiotic solution to load the matrix pores with a maximum of drug and to release large quantities of antibiotics quickly. Through these various opportunities to sample loading, it is possible to provide a wide range of different release behaviours and to select the most appropriate for each individual clinical case.

5. Conclusion

The results of this study confirmed that calcium phosphate beads obtained by ionotropic gelation are feasible as antibacterial drug carrier.

On this occasion, the initial vancomycin concentration used for loading had a greater impact on the duration of antibiotics released (5 days for 100 mg/ml compared to 3 days for 10 mg/ml), and thus the antibacterial efficacy, than the calcium phosphate powder (4 to 5 days for HAP compared to 3 to 4 days for TCP) or the utilised sintering temperature, where no differences between non-sintered beads and beads sintered at 800 °C could be measured. Nevertheless, the choice of the ceramic powder and the sintering temperature influenced, among other things, the degradation rate or the loadable drug amount. TCP beads sintered at 800 °C degrade six times faster than HAP beads sintered at 1200 °C in 14 days. Non-sintered beads load $\sim 55 \text{ mg/g}$ more vancomycin than beads sintered at 800 °C. Through the incorporation of loaded beads in a scaffold matrix by means of freeze gelation process, a spreading of the beads at the implantation site can be prevented and the duration of release and thus the duration of antibacterial activity can be further prolonged up to 1 day. By a multi-loading not only of the beads but also of the matrix, the release behaviour can be prolonged up to nearly 1 week and adjusted even more precisely. The results affirmed that composites of highly drug loaded ceramic beads incorporated in also drug loaded freeze-gelated matrix scaffolds can cause a sustained antibiotic release and antibacterial activity.

Supplementary data to this article can be found online at <http://dx.doi.org/10.1016/j.jmsec.2016.05.042>.

Acknowledgments

We kindly acknowledge Thomas Schumacher for his support with the XRD measurements, Tina Kuehn for her support with the mercury intrusion, as well as Nina Wurzler and Sebastian Hill for their support with the degradation behaviour analysis.

References

- [1] M. Baltensperger, G. Eyrich, *Osteomyelitis of the Jaws*, Springer-Verlag, Berlin, Heidelberg, 2009.
- [2] D.P. Lew, F.A. Waldvogel, *Osteomyelitis*, *Lancet* 364 (2004) 369–379.
- [3] M.S. Butler, M.A. Cooper, *Antibiotics in the clinical pipeline in 2011*, *J. Antibiot. (Tokyo)* 64 (2011) 413–425.
- [4] Y.S. Brin, J. Golenser, B. Mizrahi, G. Maoz, A.J. Domb, S. Peddada, S. Tuvia, A. Nyska, M. Nyska, *Treatment of osteomyelitis in rats by injection of degradable polymer releasing gentamicin*, *J. Control. Release* 131 (2008) 121–127.
- [5] M.Y. Krasko, J. Golenser, A. Nyska, M. Nyska, Y.S. Brin, A.J. Domb, *Gentamicin extended release from an injectable polymeric implant*, *J. Control. Release* 117 (2007) 90–96.
- [6] C. Kaehling, P. Streckbein, D. Schermund, M. Henrich, D. Burchert, S. Gattenloehner, H.P. Howaldt, J.F. Wilbrand, *Lethal cervical abscess following bisphosphonate related osteonecrosis of the jaw*, *J. Craniomaxillofac. Surg.* 42 (2014) 1203–1206.
- [7] M. Baro, E. Sanchez, A. Delgado, A. Perera, C. Evora, *In vitro-in vivo characterization of gentamicin bone implants*, *J. Control. Release* 83 (2002) 353–364.
- [8] S. Harbarth, S.L. Pestotnik, J.F. Lloyd, J.P. Burke, M.H. Samore, *The epidemiology of nephrotoxicity associated with conventional amphotericin B therapy*, *Am. J. Med.* 111 (2001) 528–534.
- [9] H.F. Chambers, *The changing epidemiology of Staphylococcus aureus?* *Emerg. Infect. Dis.* 7 (2001) 178–182.
- [10] J.D. Bryers, *Medical biofilms*, *Biotechnol. Bioeng.* 100 (2008) 1–18.
- [11] U. Gbureck, E. Vorndran, F.A. Muller, J.E. Barralet, *Low temperature direct 3D printed bioceramics and biocomposites as drug release matrices*, *J. Control. Release* 122 (2007) 173–180.
- [12] R.M. Donlan, *Biofilms and device-associated infections*, *Emerg. Infect. Dis.* 7 (2001) 277–281.
- [13] J. Ciampolini, K.G. Harding, *Pathophysiology of chronic bacterial osteomyelitis. Why do antibiotics fail so often?* *Postgrad. Med. J.* 76 (2000) 479–483.
- [14] D. Arcos, M. Vallet-Regi, *Bioceramics for drug delivery*, *Acta Mater.* 61 (2013) 890–911.
- [15] S. Bose, S. Tarafder, *Calcium phosphate ceramic systems in growth factor and drug delivery for bone tissue engineering: a review*, *Acta Biomater.* 8 (2012) 1401–1421.
- [16] S. Gitelis, G.T. Brebach, *The treatment of chronic osteomyelitis with a biodegradable antibiotic-impregnated implant*, *J. Orthop. Surg. (Hong Kong)* 10 (2002) 53–60.
- [17] H.I. Chang, Y. Perrie, A.G. Coombes, *Delivery of the antibiotic gentamicin sulphate from precipitation cast matrices of polycaprolactone*, *J. Control. Release* 110 (2006) 414–421.
- [18] D.J. Moojen, B. Hentenaar, H. Charles Vogely, A.J. Verbout, R.M. Castelein, W.J. Dhert, *In vitro release of antibiotics from commercial PMMA beads and articulating hip spacers*, *J. Arthroplast.* 23 (2008) 1152–1156.

- [19] H. van de Belt, D. Neut, D.R. Uges, W. Schenk, J.R. van Horn, H.C. van der Mei, H.J. Busscher, Surface roughness, porosity and wettability of gentamicin-loaded bone cements and their antibiotic release, *Biomaterials* 21 (2000) 1981–1987.
- [20] J.T. Mader, J. Calhoun, J. Cobos, In vitro evaluation of antibiotic diffusion from antibiotic-impregnated biodegradable beads and polymethylmethacrylate beads, *Antimicrob. Agents Chemother.* 41 (1997) 415–418.
- [21] A. Bistolfi, G. Massazza, E. Verne, A. Masse, D. Deledda, S. Ferraris, M. Miola, F. Galetto, M. Crova, Antibiotic-loaded cement in orthopedic surgery: a review, *ISRN Orthop.* 2011 (2011) 290851.
- [22] G. Lewis, Properties of antibiotic-loaded acrylic bone cements for use in cemented arthroplasties: a state-of-the-art review, *J. Biomed. Mater. Res. B Appl. Biomater.* 89 (2009) 558–574.
- [23] R.E. Barth, H.C. Vogely, A.I. Hoepelman, E.J. Peters, 'To bead or not to bead?' Treatment of osteomyelitis and prosthetic joint-associated infections with gentamicin bead chains, *Int. J. Antimicrob. Agents* 38 (2011) 371–375.
- [24] D.A. Wininger, R.J. Fass, Antibiotic-impregnated cement and beads for orthopedic infections, *Antimicrob. Agents Chemother.* 40 (1996) 2675–2679.
- [25] L. Bunetel, A. Segui, M. Cormier, E. Percheron, F. Langlais, Release of gentamicin from acrylic bone cement, *Clin. Pharmacokinet.* 17 (1989) 291–297.
- [26] S.M. Sanicola, S.F. Albert, The in vitro elution characteristics of vancomycin and tobramycin from calcium sulfate beads, *J. Foot Ankle Surg.* 44 (2005) 121–124.
- [27] J.S. Gogia, J.P. Meehan, P.E. Di Cesare, A.A. Jamali, Local antibiotic therapy in osteomyelitis, *Semin. Plast. Surg.* 23 (2009) 100–107.
- [28] X. Yang, L. Osagie, M.P. Bostrom, In vitro elution characteristics of vancomycin in a composite calcium phosphate/calcium sulfate bone substitute, *HSS J.* 8 (2012) 129–132.
- [29] B.M. Scharer, S.M. Sanicola, The in vitro elution characteristics of vancomycin from calcium phosphate-calcium sulfate beads, *J. Foot Ankle Surg.* 48 (2009) 540–542.
- [30] D. von Stechow, M. Rauschmann, Effectiveness of combination use of antibiotic-loaded PerOssal(R) with spinal surgery in patients with spondylodiscitis, *Eur. Surg. Res.* 43 (2009) 298–305.
- [31] M.A. Rauschmann, T.A. Wichelhaus, V. Stimal, E. Dingeldein, L. Zichner, R. Schnettler, V. Alt, Nanocrystalline hydroxyapatite and calcium sulphate as biodegradable composite carrier material for local delivery of antibiotics in bone infections, *Biomaterials* 26 (2005) 2677–2684.
- [32] M. Bohner, L. Galea, N. Doebelin, Calcium phosphate bone graft substitutes: failures and hopes, *J. Eur. Ceram. Soc.* 32 (2012) 2663–2671.
- [33] U. Joosten, A. Joist, G. Gosheger, U. Liljenqvist, B. Brandt, C. von Eiff, Effectiveness of hydroxyapatite-vancomycin bone cement in the treatment of *Staphylococcus aureus* induced chronic osteomyelitis, *Biomaterials* 26 (2005) 5251–5258.
- [34] B. Li, K.V. Brown, J.C. Wenke, S.A. Guelcher, Sustained release of vancomycin from polyurethane scaffolds inhibits infection of bone wounds in a rat femoral segmental defect model, *J. Control. Release* 145 (2010) 221–230.
- [35] T. Sasaki, Y. Ishibashi, H. Katano, A. Nagumo, S. Toh, In vitro elution of vancomycin from calcium phosphate cement, *J. Arthroplast.* 20 (2005) 1055–1059.
- [36] U. Hess, S. Hill, L. Treccani, P. Streckbein, K. Rezwan, A mild one-pot process for synthesising hydroxyapatite/biomolecule bone scaffolds for sustained and controlled antibiotic release, *Biomed. Mater.* 10 (2015) 015013.
- [37] M. Colilla, M. Manzano, M. Vallet-Regi, Recent advances in ceramic implants as drug delivery systems for biomedical applications, *Int. J. Nanomedicine* 3 (2008) 403–414.
- [38] X. Lian, H. Liu, X. Wang, S. Xu, F. Cui, X. Bai, Antibacterial and biocompatible properties of vancomycin-loaded nano-hydroxyapatite/collagen/poly (lactic acid) bone substitute, *Prog. Nat. Sci.* 23 (2013) 549–556.
- [39] V. Cauda, B. Onida, B. Platschek, L. Muhlstein, T. Bein, Large antibiotic molecule diffusion in confined mesoporous silica with controlled morphology, *J. Mater. Chem.* 18 (2008) 5888–5899.
- [40] J.C. Barna, D.H. Williams, The structure and mode of action of glycopeptide antibiotics of the vancomycin group, *Annu. Rev. Microbiol.* 38 (1984) 339–357.
- [41] A. Shukla, R.C. Fuller, P.T. Hammond, Design of multi-drug release coatings targeting infection and inflammation, *J. Control. Release* 155 (2011) 159–166.
- [42] H. Winkler, O. Janata, C. Berger, W. Wein, A. Georgopoulos, In vitro release of vancomycin and tobramycin from impregnated human and bovine bone grafts, *J. Antimicrob. Chemother.* 46 (2000) 423–428.
- [43] V. Antoci Jr., C.S. Adams, N.J. Hickok, I.M. Shapiro, J. Parvizi, Antibiotics for local delivery systems cause skeletal cell toxicity in vitro, *Clin. Orthop. Relat. Res.* 462 (2007) 200–206.
- [44] T.Y. Klein, L. Treccani, K. Rezwan, Ceramic microbeads as adsorbents for purification technologies with high specific surface area, adjustable pore size, and morphology obtained by ionotropic gelation, *J. Am. Ceram. Soc.* 95 (2012) 907–914.
- [45] B. Mueller, D. Koch, R. Lutz, K.A. Schlegel, L. Treccani, K. Rezwan, A novel one-pot process for near-net-shape fabrication of open-porous resorbable hydroxyapatite/protein composites and in vivo assessment, *Mater. Sci. Eng. C* 42 (2014) 137–145.
- [46] S. Brunauer, P.H. Emmett, E. Teller, Adsorption of gases in multimolecular layers, *J. Am. Ceram. Soc.* 60 (1938) 309–319.
- [47] G. Hanlon, N. Hodges, *Essential Microbiology for Pharmacy and Pharmaceutical Science*, Wiley-Blackwell, Chichester, West Sussex, U.K., 2013.
- [48] J. McFarland, The nephelometer - an instrument for estimating the number of bacteria in suspensions used for calculating the opsonic index and for vaccines, *J. Am. Med. Assoc.* 49 (1907) 1176–1178.
- [49] T. Ostberg, L. Vesterhus, C. Graffner, Calcium alginate matrices for oral multiple unit administration: II. Effect of process and formulation factors on matrix properties, *Int. J. Pharm.* 97 (1993) 183–193.
- [50] A.Y. Mateus, C.C. Barrias, C. Ribeiro, M.P. Ferraz, F.J. Monteiro, Comparative study of nano-hydroxyapatite microspheres for medical applications, *J. Biomed. Mater. Res. A* 86 (2008) 483–493.
- [51] T.C. Schumacher, T.Y. Klein, L. Treccani, K. Rezwan, Rapid sintering of porous mono-liths assembled from microbeads with high specific surface area and multimodal porosity, *Adv. Eng. Mater.* 16 (2014) 151–155.
- [52] M. Pulkin, D. Koch, G. Grathwohl, Silica effect on porous calcium phosphate ceramics from the freeze gelation route, *Int. J. Appl. Ceram. Technol.* 8 (2011) 1414–1424.
- [53] X.W. Li, H.Y. Yasuda, Y. Umakoshi, Bioactive ceramic composites sintered from hydroxyapatite and silica at 1200 °C: preparation, microstructures and in vitro bone-like layer growth, *J. Mater. Sci. Mater. Med.* 17 (2006) 573–581.
- [54] J.W. Reid, A. Pietak, M. Sayer, D. Dunfield, T.J. Smith, Phase formation and evolution in the silicon substituted tricalcium phosphate/apatite system, *Biomaterials* 26 (2005) 2887–2897.
- [55] C.P. Klein, J.M. de Bleeck-Hogervorst, J.G. Wolke, K. de Groot, Studies of the solubility of different calcium phosphate ceramic particles in vitro, *Biomaterials* 11 (1990) 509–512.
- [56] R.Z. LeGeros, Biodegradation and bioresorption of calcium phosphate ceramics, *Clin. Mater.* 14 (1993) 65–88.
- [57] K. Potter, B.J. Balcom, T.A. Carpenter, L.D. Hall, The gelation of sodium alginate with calcium ions studied by magnetic resonance imaging (MRI), *Carbohydr. Res.* 257 (1994) 117–126.
- [58] A. Blandino, M. Macias, D. Cantero, Formation of calcium alginate gel capsules: influence of sodium alginate and CaCl₂ concentration on gelation kinetics, *J. Biosci. Bioeng.* 88 (1999) 686–689.
- [59] C. Klein, A. Driessen, K. de Groot, A. van den Hooff, Biodegradation behavior of various calcium phosphate materials in bone tissue, *J. Biomed. Mater. Res.* 17 (1983) 769–784.
- [60] M. Stigter, J. Bezemer, K. de Groot, P. Layrolle, Incorporation of different antibiotics into carbonated hydroxyapatite coatings on titanium implants, release and antibiotic efficacy, *J. Control. Release* 99 (2004) 127–137.
- [61] S. Deville, Ice-templating, freeze casting: beyond materials processing, *J. Mater. Res.* 28 (2013) 2202–2219.
- [62] W.L. Li, K. Lu, J.Y. Walz, Freeze casting of porous materials: review of critical factors in microstructure evolution, *Int. Mater. Rev.* 57 (2012) 37–60.
- [63] D.M. Citron, M.D. Appleman, In vitro activities of daptomycin, ciprofloxacin, and other antimicrobial agents against the cells and spores of clinical isolates of bacillus species, *J. Clin. Microbiol.* 44 (2006) 3814–3818.
- [64] C. Fang, E. Stiegeler, G. Cook, T. Mascher, S. Gebhard, *Bacillus subtilis* as a platform for molecular characterisation of regulatory mechanisms of *Enterococcus faecalis* resistance against cell wall antibiotics, *PLoS One* 9 (2014).



Ulrike Hess initially studied Medical Engineering and Sports Medical Engineering at the University of Applied Sciences Koblenz, Germany where she received her Diploma in 2007. Subsequently, she worked as research assistant at the Fraunhofer Technology Development Group in Stuttgart, Germany. In 2008, she started studying Biomedical Engineering at the Leibniz University Hannover, Germany and finished her studies with a Master's degree in 2010. Afterwards, she joined the Advanced Ceramics Group at the University of Bremen, Germany as a Ph.D. student. Her research focus is the development of calcium phosphate carrier for drug delivery and bone replacement.



Gerd Mikolajczyk started a course of studies in mechanical engineering at TU Dresden in 2008 which he finished in October 2013 receiving the Diplom-Ingenieur degree on the thermal and fluidic optimization of cooling fins. Since 2013 he is a member of the MIMENIMA graduate school. His research interests include the investigation of porous ceramic materials and deep bed filtration processes by means of X-ray micro-computed tomography and magnetic resonance imaging as well as the combination of both means of measurement (image registration).



Laura Treccani is Senior Researcher at Petroceramics S.p.A. (Stezzano), Italy. She earned her degree in physics from the Catholic University of Brescia, Italy, and carried out PhD thesis on biomineralization processes and interactions between nature proteins and calcium carbonate crystals. In 2006 she joined the Bioceramics Group at the Department of Process and Industrial Engineering at the University of Bremen as research fellow and till 2015 she was Vice Head of the Advanced Ceramics group at the University of Bremen, Germany. Her research is focused on the development and characterization methodologies for surface modification of ceramic materials for biomaterials bioengineering and nanotoxicological and environmental applications. She has authored more than sixty scientific publications and European patents.



Philipp Streckbein 1976 born in Weilburg, Germany. 1998–2009 studies in dentistry and medicine at the University in Mainz and Giessen, Germany. Since 2004 he worked as trainee in Oral and Cranio-Maxillo-Facial Surgery at the University hospital of the Justus-Liebig-University in Giessen. Since 2007 he is Senior Consultant in Oral Surgery and Specialist in Oral Implantology. Since 2012 he is Senior Consultant for Cranio-Maxillo-Facial Surgery, and is a Fellow of the European Board of Oral-Maxillo-Facial Surgeons (FEBOMFS). He was awarded for his scientific research in 2008 and 2010 (German association for dental implantology) and has the certification FELASA C for animal trials.



Christian Heiss is Surgery Specialist in Orthopaedics and Traumatology, Special Trauma Surgery, Sports Medicine, and Emergency Medicine. In 2006, he joined the Clinic for Trauma, Hand and Reconstructive Surgery, including Operative Emergency, at the University Hospital of Giessen-Marburg. Since 2014, he is Director of the Department of Trauma, Hand and Reconstructive Surgery. He is co-founder of the Laboratory of Experimental Traumatology at the Justus-Liebig-University of Giessen. Currently, he is also spokesman for the Collaborative Research Centre/Transregional “Materials for Hard Tissue Regeneration within Systemically Altered Bone” from the German Research Foundation (DFG) with personal research focus on osteoporosis, multiple myeloma and infection research.



Stefan Odenbach received his doctoral degree in 1993 from the University of Munich with his thesis on diffusion induced convection in magnetic fluids. He was a postdoctoral fellow at the Institute of Material Sciences BUGH in Wuppertal and at the Center of Applied Space technology and microgravity ZARM at the University of Bremen. From 2004 to 2005 he was a professor at the University of Bremen and since 2005 he is a Full Professor at TU Dresden. His research interests include the rheological characterization of magnetic fluids as well as the investigation of the microstructure of particle loaded elastomers.



Kurosch Rezwan received his PhD in Materials Science in 2005 at the ETH Zurich. After a year as visiting research fellow at the Imperial College London, he joined the University of Bremen as an Assistant Professor for Bioceramics. In 2009 he became a Full Professor of Advanced Ceramics. Between 2013 and 2015 he was also vice rector for Research and Young Academics at the University of Bremen. He serves as referee for the European Research Council, the German Research Foundation, the German Parliament and for several international journals. In 2011, he received the award as the most cited scientific article in the biomaterials field for the years 2006–2010.